



Research paper

Seasonal trends in photosynthesis and leaf traits in scarlet oak

Angela C. Burnett^{1,2,3}, Shawn P. Serbin¹, Julien Lamour¹, Jeremiah Anderson¹,
Kenneth J. Davidson¹, Dedi Yang¹ and Alistair Rogers¹

¹Environmental and Climate Sciences Department, Brookhaven National Laboratory, Upton, NY 11973, USA; ²Present address: Department of Plant Sciences, University of Cambridge, Downing Street, Cambridge CB2 3EA, UK; ³Corresponding author (acb219@cam.ac.uk)

Received September 25, 2020; accepted January 22, 2021; handling Editor Annikki Mäkelä

Understanding seasonal variation in photosynthesis is important for understanding and modeling plant productivity. Here, we used shotgun sampling to examine physiological, structural and spectral leaf traits of upper canopy, sun-exposed leaves in *Quercus coccinea* Münchh (scarlet oak) across the growing season in order to understand seasonal trends, explore the mechanisms underpinning physiological change and investigate the impact of extrapolating measurements from a single date to the whole season. We tested the hypothesis that photosynthetic rates and capacities would peak at the summer solstice, i.e., at the time of peak photoperiod. Contrary to expectations, our results reveal a late-season peak in both photosynthetic capacity and rate before the expected sharp decrease at the start of senescence. This late-season maximum occurred after the higher summer temperatures and vapor pressure deficit and was correlated with the recovery of leaf water content and increased stomatal conductance. We modeled photosynthesis at the top of the canopy and found that the simulated results closely tracked the maximum carboxylation capacity of Rubisco. For both photosynthetic capacity and modeled top-of-canopy photosynthesis, the maximum value was therefore not observed at the summer solstice. Rather, in each case, the measurements at and around the solstice were close to the overall seasonal mean, with values later in the season leading to deviations from the mean by up to 41 and 52%, respectively. Overall, we found that the expected Gaussian pattern of photosynthesis was not observed. We conclude that an understanding of species- and environment-specific changes in photosynthesis across the season is essential for correct estimation of seasonal photosynthetic capacity.

Keywords: gas exchange, leaf traits, phenology, physiology, temporal changes, $V_{c,max}$.

Introduction

Photosynthesis underpins primary productivity on Earth. Understanding photosynthesis is essential for developing accurate terrestrial biosphere models (TBMs), which aim to represent the responses of plants to future climate and the role plants play in determining the rate of global change. Accounting for temporal and spatial variation in photosynthesis is critical if TBMs are to accurately predict carbon fluxes across space and through time. For example, under-representation of photosynthetic understanding due to an absence of relevant data in certain geographical areas, such as Arctic ecosystems, can lead to significant biases in model predictions (e.g., Rogers et al. 2017). To address the constraint of limited data availability for parameterization, some TBMs use nitrogen as a proxy

for photosynthesis, yet the relationship between nitrogen and photosynthesis has been shown to vary by plant functional type (Kattge et al. 2009), making this challenging. In addition, consideration of seasonal changes is important given that photosynthetic capacity has been shown to display significant variation during the growing season (Wilson et al. 2001, Wang et al. 2008, Bauerle et al. 2012, Ali et al. 2015). Environmental parameters such as photoperiod and growth temperature may explain this seasonal variation in photosynthetic capacity, since climatic conditions have been demonstrated to be a better proxy for photosynthesis than leaf nitrogen (Ali et al. 2015, Smith et al. 2019). For example, a recent study of 23 tree species found that photoperiod was the primary environmental driver for seasonal changes in photosynthetic capacity—both

the maximum carboxylation capacity of Rubisco ($V_{c,max}$) and the maximum electron transport rate (J_{max}) (Bauerle et al. 2012). However, the extent to which different environmental conditions underpin photosynthetic rate can vary between species and ecosystems studied, with temperature, moisture availability and atmospheric humidity being other important environmental factors to consider (Ali et al. 2015).

The $A-C_i$ response curves measure the response of photosynthesis (A) to the internal CO_2 concentration inside the leaf (C_i). With these curves, it is possible to derive the estimates of the apparent maximum carboxylation capacity of Rubisco ($V_{c,max}$) and apparent maximum electron transport rate (J_{max}), two key parameters related to photosynthetic capacity (Long and Bernacchi 2003). However, obtaining accurate measurements of photosynthetic capacity in tree species is not without its challenges. The ideal scenario, performing measurements *in situ* while preserving the water column to the leaf and maintaining ambient environmental conditions, requires expensive aerial work platforms such as 'cherry-pickers' or canopy cranes (Wu et al. 2019). Lower cost and more logistically feasible solutions involve retrieving samples from the canopy for subsequent measurement. There exist a range of approaches for retrieving canopy samples, including line launchers, sling shots or air cannons (Serbin et al. 2014); for samples lower in the canopy, pruning poles are often sufficient (Kamoske et al. 2020). If retrieval times are lengthy, leading to a long sample collection period, this can result in sample deterioration. The shotgun sampling approach, using a shotgun to retrieve leaf samples (Burnett et al. 2019, Serbin et al. 2014), enables rapid acquisition of plant material from the top of the canopy. Collecting and stabilizing each sample takes a matter of minutes, enabling the rapid acquisition of a set of samples within a short-time period. This means that all samples may be collected at dawn, before photosynthetic activity begins to acclimate to the day's conditions, and ensures that leaf quality is maintained throughout the measurement period due to the speed of sample collection.

We sought to understand the seasonal variation in physiological and structural leaf traits in *Quercus coccinea* (scarlet oak) in the mid-Atlantic region using the shotgun sampling approach. We performed regular measurements throughout the entire growing season and examined the relationships between physiological traits, structural traits, leaf nitrogen and leaf chlorophyll to (i) understand seasonal trends, (ii) explore the mechanisms underpinning physiological change and (iii) investigate the impact of extrapolating measurements made at a single time point when deriving parameters for use in TBMs. In accordance with previous studies (Bauerle et al. 2012, Wilson et al. 2001), we hypothesized that photosynthetic rates and capacities would be greatest at the midsummer solstice (day of year (DOY) 172) when photoperiod is at its peak, meaning that a midsummer measurement would provide a significant

overestimation of mean photosynthesis if used as a model parameter.

Materials and methods

Tree material

Quercus coccinea Muench (scarlet oak) samples were obtained from a mixed pine-oak forest at Brookhaven National Laboratory, Upton, NY, USA (latitude 40.864466, longitude 72.875158, 18-m elevation). Scarlet oak is a native, deciduous, xerophytic tree with an open, rounded crown (USDA 2019). The study site is part of the Long Island Pine Barrens, characterized by dry sandy soils (Meng et al. 2017). Six trees were selected at the start of the measurement season and labeled with flagging tape to enable repeated measurements. The trees were located in a small geographic area (<30-m radius). Each tree selected displayed a mature canopy structure, so that sampling could be repeated for the duration of the experiment with minimal adverse effects.

Meteorological data

Meteorological data were obtained from the Brookhaven National Laboratory meteorological data service (www.bnl.gov/weather/). Solar data were converted to photosynthetically active radiation by multiplying $W\ m^{-2}$ by 2.1. Vapor pressure deficit (VPD) was obtained from temperature and relative humidity data using the 'Bigleaf' package in R (Knauer et al. 2018).

Shotgun sampling technique

Leaf samples were collected at dawn. Samples from the top of the canopy were retrieved using shotgun sampling (Burnett et al. 2019, Serbin et al. 2014). A 12-gauge Remington 870 Express Pump-Action Shotgun with a modified choke and stainless-steel bird shot was used to retrieve canopy samples (Figure 1a). Each sample comprised several leaves, and a small amount of connecting woody material (Figure 1b). The woody stem of each sample was immediately recut under water (within 2 min) and was kept in water until the completion of physiological data collection. Samples were kept in individual bottles of water. Once all samples had been collected (typically < 1 h), samples were transferred from the forest to the laboratory for data collection.

Measurement schedule

Data were collected in 2019 throughout the entire growing season of *Q. coccinea*. The first sampling date occurred when leaves were sufficiently expanded for measurement, i.e., within a couple of weeks of leaf flushing, and the last sampling date occurred at the onset of senescence, with leaves turning scarlet on the trees. There were eight sampling dates (Figure 2), beginning on DOY 149 (late May) and ending on DOY 303 (late



Figure 1. Shotgun sampling technique for retrieving leaf samples of *Q. coccinea*. (a) A shotgun was used to obtain a sample from the top of the canopy. (b) Stems were re-cut underwater and samples stored on the forest floor until sample collection was complete. (c) Following physiological data collection, leaf discs were punched out of the leaf; discs were used in subsequent measurements of structural traits and leaf nitrogen.

October). Gas exchange measurements were collected on seven of the eight sampling dates; all leaf trait data were collected on each sampling date with the exception of one date for which no relative water content (RWC) values could be calculated.

Chlorophyll and PRI

For each sample, spectral data were collected using a PSR+ full-range spectroradiometer (Spectral Evolution, Lawrence, MA, USA) connected to a leaf clip with an internal light source (SVC, Poughkeepsie, NY, USA). Immediately prior to each set of measurements, the spectroradiometer was calibrated using a LabSphere Spectralon® reflectance standard disc (LabSphere, Inc., North Sutton, NH, USA). Two to three spectral measurements were taken across the adaxial surface of each leaf depending on leaf size, and then averaged to give a single spectrum per sample. Chlorophyll was estimated from each spectrum using the Chlorophyll NDI index. The index was derived from using the formula $(R_{750} - R_{705}) / (R_{750} + R_{705})$ where R is optical reflectance at the waveband indicated and chlorophyll content was estimated using the conversion equation provided by Richardson et al. (2002). The photochemical reflectance index (PRI) was estimated from each spectrum using the formula $(R_{531} - R_{570}) / (R_{531} + R_{570})$ (Gamon et al. 1997).

Gas exchange measurements

Gas exchange measurements were performed using four LI-6400XT Portable Photosynthesis Systems and one LI-6800 Portable Photosynthesis System (LI-COR, Lincoln, NE, USA). Instruments were zeroed using a common nitrogen

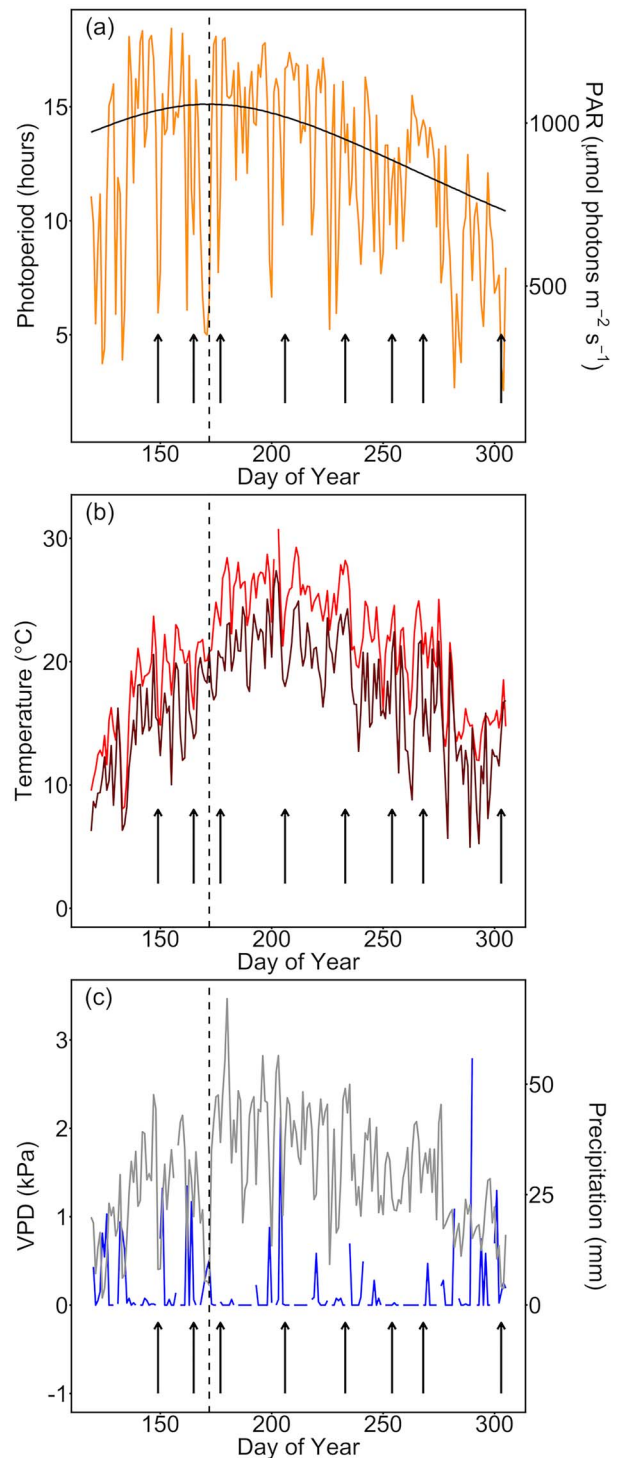


Figure 2. Meteorological data throughout the sampling period, beginning 30 days before the first measurement. Sampling dates are indicated with vertical black arrows and the midsummer solstice is indicated with a vertical black dashed line. (a) Photoperiod (solid black line; primary y-axis) and mean daytime PAR on each measurement date (yellow line; secondary y-axis). (b) Mean daytime temperature (bright red line) and nighttime temperature (dark red line). (c) Maximum daily VPD (gray line; primary y-axis) and total daily precipitation (bright blue line; secondary y-axis).

standard. In the preceding season, light response curves had been performed to determine the saturating irradiance level of $1500 \mu\text{mol photons m}^{-2} \text{s}^{-1}$ for *Q. coccinea* (Burnett et al. 2019). The leaf temperature was controlled during measurement and the set point was determined by the ambient temperature and humidity inside the laboratory at the time of measurement (the temperature ranged from 22 to 28 °C). Leaves were inserted into the instrument leaf chamber and underwent full acclimation to saturating light (up to 90 min) until both A and stomatal conductance (g_s) had reached steady-state. The $A-C_i$ curves were performed as described previously, using 14 values of C_i (Burnett et al. 2019, Rogers et al. 2017). Values of $V_{c,\text{max}}$ and J_{max} were first obtained by fitting the $A-C_i$ curves using the parameters defined by Bernacchi et al. (Bernacchi et al. 2001, 2013, Rogers et al. 2017). Values of $V_{c,\text{max}}$ and J_{max} were then normalized to 25 °C with an Arrhenius temperature scaling function using activation energies provided by Bernacchi et al. (2001, 2003), to give $V_{c,\text{max},25}$ and $J_{\text{max},25}$. Efforts to increase the representation of $V_{c,\text{max}}$ using survey-style measurements of photosynthesis to increase the availability of data from existing databases or to increase the throughput of data collection are not always reliable if leaves were not light-acclimated prior to measurement (Burnett et al. 2019, De Kauwe et al. 2016). Therefore, while being more time-consuming to perform than a survey-style measurement, $A-C_i$ curves remain the gold-standard approach for measuring photosynthetic capacity. Our analysis is based on C_i rather than C_c and therefore does not account for mesophyll conductance. Thus, reported photosynthetic parameters should be considered as apparent.

Gas exchange measurements were used to derive photosynthetic instantaneous water-use efficiency (WUEi) and photosynthetic nitrogen-use efficiency (NUE). The WUEi is light-acclimated steady-state A_{sat}/g_s obtained from the first point of each $A-C_i$ curve. The NUE is $V_{c,\text{max},25}/N$, both expressed on a mass basis; mass-based $V_{c,\text{max}}$ was first obtained from area-based $V_{c,\text{max},25}$ and leaf mass per unit area (LMA).

Gas exchange measurements were also used to calibrate the conductance model needed for modeling photosynthesis. To obtain the stomatal slope parameter g_1 , which is the slope of the relationship between A and g_s and is required for modeling photosynthesis as outlined below, the first point of each $A-C_i$ curve was recorded after initial stabilization of A and g_s and acclimation to ambient conditions inside the leaf cuvette. For each measurement date, the first points from all $A-C_i$ curves were pooled, and the g_1 parameter from the simplified linear USO model (Eq. (1)) was obtained using a linear regression as shown previously (Lin et al. 2015, Medlyn et al. 2011, Wu et al. 2020), using a default g_0 of 0

$$g_{\text{sw}} = g_0 + g_1 \frac{1.6 A_n}{C_s \sqrt{D_s}}, \quad (1)$$

where g_{sw} is the stomatal conductance to water vapor, g_0 and g_1 are the intercept and the slope of the linear regression,

respectively, A_n is net CO_2 assimilation, C_s is CO_2 at the surface of the leaf (C_a) and D_s is leaf to air VPD. For the first measurement date, a good estimate of g_1 could not be obtained so the mean g_1 from all other dates (except the final date for which g_1 was much higher than on all preceding dates) was used instead.

Leaf structural and nitrogen trait measurements

Following the completion of each $A-C_i$ curve, discs of known area were punched from across the leaf surface, including the area used for gas exchange and excluding the prominent lower midrib (Figure 1c). Leaf discs were weighed, then dried at 70 °C for several days to achieve constant mass. Dried leaves were re-weighed, and RWC and LMA were calculated. Dried leaves were subsequently ground, and elemental nitrogen was quantified using a 2400 Series II CHN analyzer following the manufacturer's instructions (PerkinElmer, Waltham, MA, USA).

Data analysis

All data analysis was performed within the R open-source software environment (R Core Team 2019). For analysis of each leaf trait (Figures 3 and 4), a one-way repeated measures ANOVA was performed to examine effects over time, with the individual tree as the Error term. A post hoc Tukey test was then performed to examine pairwise comparisons between each possible pair of measurement dates. When required, data were log- or square-root-transformed prior to analysis as appropriate.

Modeling photosynthesis

Photosynthesis at the top of the canopy was modeled for each measurement date using the *fAT* function within the 'Leaf Gas Exchange' package in R (<https://github.com/TESTgroup-BNL/LeafGasExchange/releases/tag/v1.0>). This function simulates photosynthesis using the simplified USO model coupled with the FvCB assimilation model and a leaf energy budget (Muir 2019). The inputs to the model are the ambient atmospheric weather conditions surrounding the leaves (photosynthetically active radiation, air temperature, CO_2 concentration at the leaf surface, wind speed and relative humidity), the photosynthetic parameters R_d , $V_{c,\text{max},25}$, $J_{\text{max},25}$ and the conductance parameters g_0 and g_1 . The outputs are A , g_{sw} , C_i and T_{leaf} . The function *fAT* was parameterized using $V_{c,\text{max},25}$, $J_{\text{max},25}$, g_0 and g_1 calibrated using the data from this study. For the other parameters necessary to calculate photosynthesis, including R_d , the default parameters used in the Functionally Assembled Terrestrial Ecosystem Simulator (Koven et al. 2020) for C_3 plant species were chosen. The weather input variables were set to the mean weather data measured during the week of each sampling date (measurement date ± 3 days) during the 6-h period around solar noon (10:00–16:00h BST), and CO_2 at the leaf surface was set to $400 \mu\text{mol mol}^{-1}$.

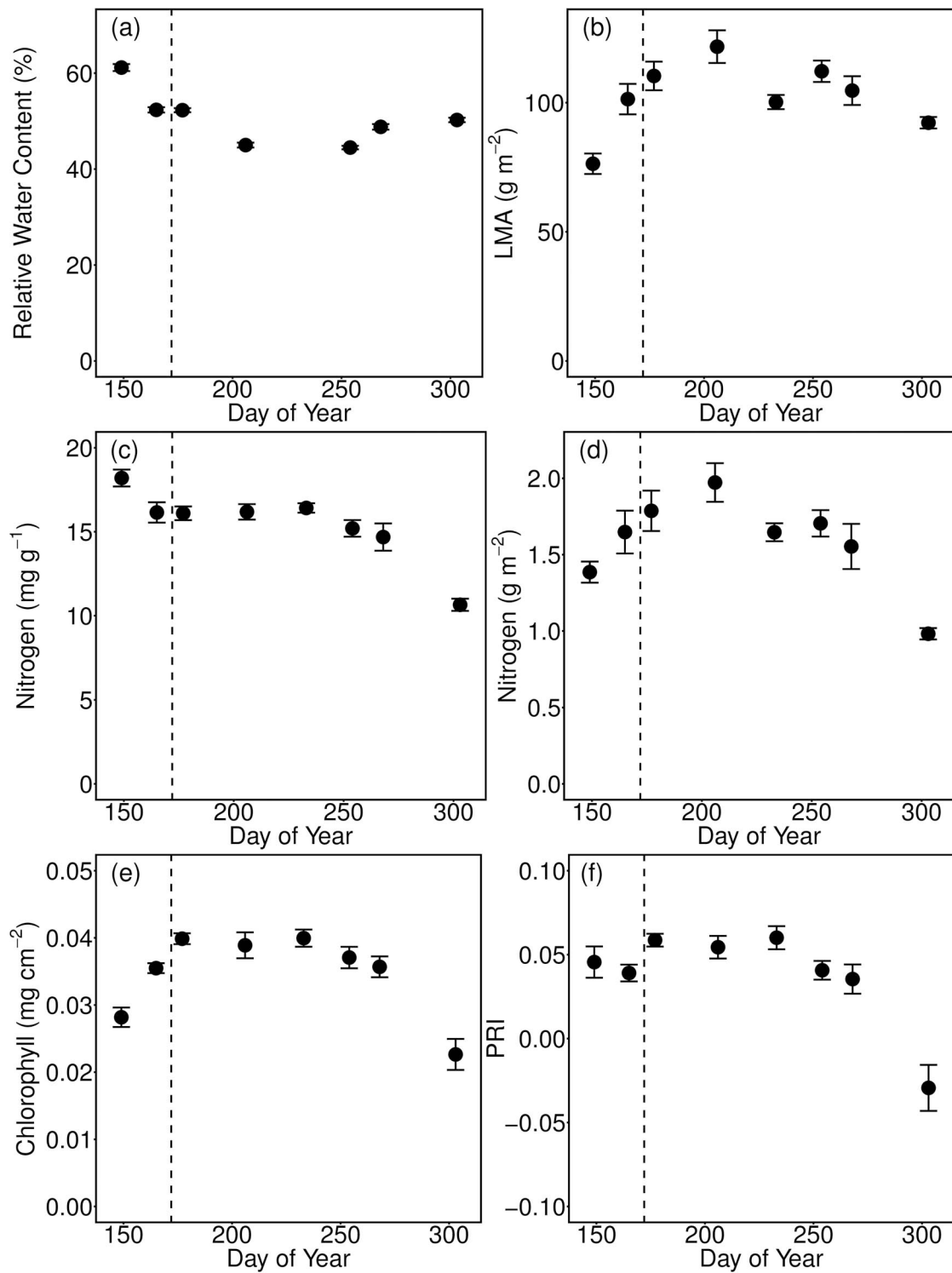


Figure 3. Seasonal trends in leaf structural traits, nitrogen, chlorophyll and PRI. The midsummer solstice is indicated with a dashed line. (a) RWC; (b) LMA; (c) leaf nitrogen concentration per gram; (d) leaf nitrogen content per m^2 ; (e) chlorophyll estimated using a leaf reflectance index; (f) PRI. Plots show mean \pm SE, $n = 6$ trees.

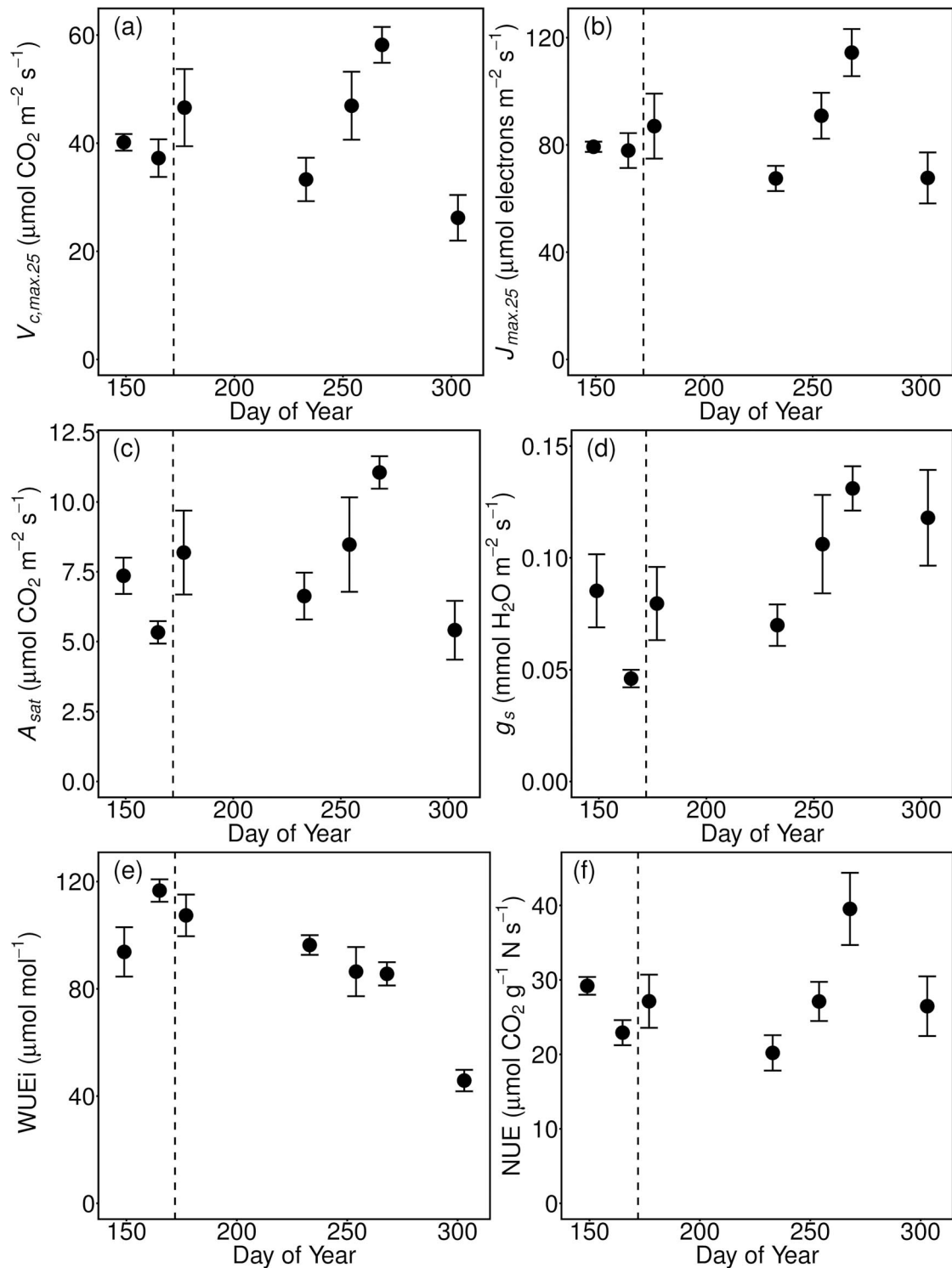


Figure 4. Seasonal trends in photosynthetic traits. The midsummer solstice is indicated with a dashed line. (a) Maximum carboxylation capacity of Rubisco normalized to 25 °C, $V_{c,max,25}$; (b) maximum electron transport rate normalized to 25 °C, $J_{max,25}$; (c) light-saturated photosynthesis, A_{sat} , measured immediately prior to the $A-C_i$ curve; (d) light-acclimated stomatal conductance, g_s , measured immediately prior to the $A-C_i$ curve; (e) instantaneous water-use efficiency, WUEi; (f) NUE of photosynthesis. Plots show mean \pm SE, $n = 6$ trees.

Results

Leaf structural traits

The RWC and LMA showed inverse relationships to each other (Figure 3). Relative water content was initially very high, declined in the middle of the season and then increased toward the end of the season; LMA was initially very low, increased toward the middle of the season and declined again at the end of the season. In each case, trait values differed significantly over time (RWC $F_{(6,30)} = 185.8$, $P < 0.001$; LMA $F_{(7,35)} = 11.1$, $P < 0.001$). Pairwise comparisons revealed a significant difference in RWC between all possible measurement date pairs with the exception of the pairs DOY 165–177 (stabilization of RWC around the solstice), 254–303 and 268–303 (stabilization at the end of the season). For LMA, there was a significant difference for the following pairs of measurement dates: DOY 149–165, 149–177, 149–206, 149–233, 149–254, 149–268, 165–206, 206–233, 206–303 and 254–303, in line with the strong and significant increase at the beginning of the season, a dip between DOY 206 and 233 and the decline toward the end of the season. The reporting format 'DOY1'–'DOY2' used here indicates a significant difference between the two named DOYs and does not refer to a date range.

Leaf nitrogen and chlorophyll

When expressed on a leaf mass basis, nitrogen concentration was initially high, was stable throughout much of the season and then gradually declined over the last three measurement dates (Figure 3). When expressed on a leaf area basis, nitrogen showed a steady increase followed by a steady decrease, with a sharp decline to the final time point, closely following the trend in LMA (Figure 3). Leaf chlorophyll and PRI showed similar trends to nitrogen per unit area (Figure 3). Trends in each trait showed significant effects of time (mass-based nitrogen $F_{(7,35)} = 20.1$, $P < 0.001$; area-based nitrogen $F_{(7,35)} = 10.2$, $P < 0.001$; chlorophyll $F_{(7,35)} = 15.3$, $P < 0.001$; PRI $F_{(7,35)} = 14.0$, $P < 0.001$). For mass-based nitrogen, significant differences were observed for the date pairs 149–254, 149–268 and between the final measurement date (DOY 303) and each preceding date. For area-based nitrogen, significant differences were observed between DOY 149 and 206 and between the final measurement date (DOY 303) and each preceding date, with the exception of DOY 149 and 303 which did not differ significantly. For chlorophyll, there was a significant difference between the first measurement date (DOY 149) and all subsequent dates with the exception of DOY 303, and there was a significant difference between the final measurement date (DOY 303) and each of the preceding dates with the exception of DOY 149. For PRI, there were significant differences between DOY 303 and each of the preceding dates.

Photosynthetic traits

The derived photosynthetic parameters $V_{c,max,25}$, $J_{max,25}$ and light-acclimated net photosynthetic rate A_{sat} showed similar trends (Figure 4) with a significant effect of time in each case ($V_{c,max,25}$ $F_{(6,29)} = 5.2$; $P < 0.001$; $J_{max,25}$ $F_{(6,26)} = 4.2$, $P < 0.01$; A_{sat} $F_{(6,29)} = 3.7$, $P < 0.01$). These parameters all showed a late season peak (at the penultimate measurement date), followed by a sharp decline. The decline in $J_{max,25}$ between the penultimate and final time points was less marked (41%) than the equivalent decline in $V_{c,max,25}$ (55%). Stomatal conductance (g_s) measured following full acclimation to saturating irradiance, i.e., immediately prior to measuring the A–C_i response followed the same pattern as $V_{c,max,25}$, $J_{max,25}$ and A_{sat} for most of the season (g_s $F_{(6,29)} = 4.7$, $P < 0.01$), but was decoupled at the final time point which showed a very low value of A_{sat} compared with g_s (Figure 4). This trend is reflected in WUE_i, which was at the minimum at the final time point due to a low rate of A_{sat} compared with g_s (Figure 4). In contrast, photosynthetic NUE remained relatively constant throughout the measurement period, with the greatest value at the penultimate measurement date coinciding with the late-season peak in photosynthesis (Figure 4). Both WUE_i and NUE displayed significant time effects (WUE_i $F_{(6,29)} = 16.0$, $P < 0.001$; NUE $F_{(6,29)} = 4.5$, $P < 0.01$).

Pairwise comparisons made between all pairs of measurement dates revealed significant differences in $V_{c,max,25}$ between DOY 165–254, 254–268, 254–303 and 268–303, highlighting the late-season peak on DOY 268 and dramatic decline at the end of the season. Differences in $J_{max,25}$ were significant between DOY 254–268 and 254–303; differences in A_{sat} were significant between DOY 165–254, 254–268 and 254–303; differences in g_s were significant between DOY 165–254, 165–268 and 165–303; in each case, these significant differences relate to the late-season peak and subsequent decline described above. Differences in WUE_i were significant between DOY 165–233, 165–254 and 165–268, showing the decline from the maximum just before the summer solstice, and between the final measurement date (DOY 303) and each preceding date, indicating the sharp decrease in WUE at the end of the season compared with all other dates. Differences in NUE were significant between DOY 165–254 and 254–303.

Modeling photosynthesis

Using ambient environmental conditions from the week of measurement (measurement date ± 3 days) during the 6-h period around solar noon (10:00–16:00h BST), and modeled values of g_0 and g_1 , modeled values of $V_{c,max,25}$ and $J_{max,25}$ were used to predict the rate of net photosynthesis at the top of the canopy (Figure 5). Modeled photosynthesis closely matched the trend in $V_{c,max,25}$ —including the steeper decline at the final time point seen for $V_{c,max,25}$ than for $J_{max,25}$ (Figure 4).

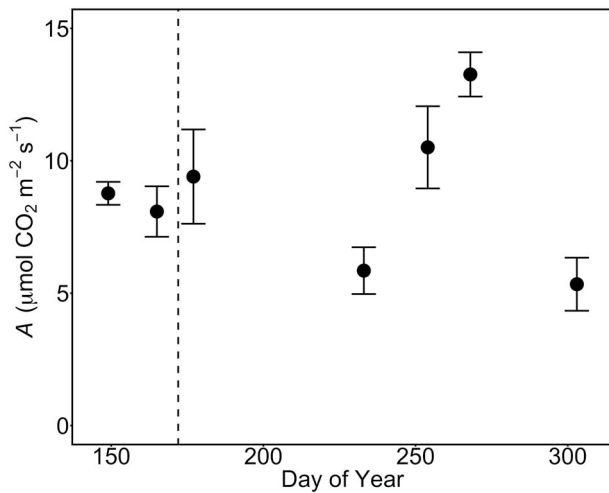


Figure 5. Photosynthesis (A) at the top of the canopy modeled from environmental data, photosynthetic capacity and stomatal slope parameters. The midsummer solstice is indicated with a dashed line. Plots show mean \pm SE, $n = 6$ trees.

Using the model framework, we further explored how seasonality in parameters could impact the modeling of growing season photosynthesis. We did this by examining the deviation from the mean in both $V_{c,max,25}$ and modeled A to explore how seasonal conditions can change the overall canopy-scale photosynthetic carbon uptake. We found that there was substantial seasonality, and variation increased throughout the season with values both greater and lower than the mean (Figure 6). In each case, the deviation was lowest at and around the midsummer solstice and greatly increased in magnitude with the late-season peak and end-season decline in photosynthesis (Figure 6). The maximum deviation from the mean was 41% for $V_{c,max,25}$ and 52% for modeled A .

Discussion

We sought to understand seasonal trends in physiological traits of *Q. coccinea*, explore the mechanisms underpinning these trends and consider the modeling implications of using single time point measurements of photosynthesis to parameterize carbon models. Our results indicate a surprising late-season maximum in photosynthesis coincident with a rise in leaf water content and stomatal conductance, lower air temperatures and an overall reduction in atmospheric VPD. In contrast to our hypothesis, photosynthetic capacity did not peak at the solstice and displayed significant deviation from the mean value later in the season.

Variability in photosynthetic capacity and rate is related to climate

Photosynthetic traits displayed great variability across the season. Similar to previous studies (e.g., Yang et al. 2016), we observed a typical Gaussian seasonal curve for traits such as

pigment content, LMA and area-based nitrogen, while mass-based nitrogen and RWC generally showed a steady decline from leaf flush to senescence. Contrary to our expectations, and in contrast to the findings of several previous studies demonstrating the seasonal Gaussian trend in photosynthesis that we had expected, with the peak at the summer solstice (Bauerle et al. 2012, Grassi et al. 2005, Kosugi and Matsuo 2006, Wilson et al. 2000, 2001), the peak in photosynthetic rate and capacity occurred late in the season, at the penultimate measurement point (Figure 4). While the amount of daylight was greatest at the midsummer solstice (Figure 2), with both the highest photosynthetically active radiation (PAR and the longest) daylength combining to give the greatest integrated daily light levels, this did not coincide with maximal photosynthetic rate. Rather, the peak in $V_{c,max,25}$, $J_{max,25}$ and A_{sat} occurred once the high summer temperatures and VPD began to decline yet before daily PAR decreased (Figures 2 and 4). This coincided with an increase in RWC (Figure 3) that followed the peak summer heat (Figure 2). While the year of measurement was slightly warmer and drier than some previous years, it was not exceptional in terms of meteorological factors (see Figure S1 available as Supplementary Data at *Tree Physiology Online*). A previous study in which *Quercus douglasii* (blue oak) was exposed to heat stress revealed a strong effect of heat on $V_{c,max,25}$; this study also showed a slight end of season peak in $V_{c,max,25}$ prior to senescence although this was not the seasonal maximum (Xu and Baldocchi 2003).

The RWC and LMA were generally inversely correlated with one another (Figure 3). At the start of the season, RWC was at its highest and LMA at its lowest as the developing leaves were thin, soft and not fully expanded at the first measurement date, which was within a couple of weeks of leaf flushing. After the solstice, as temperatures increased, RWC declined and recovered later in the season as temperatures declined (Figures 2 and 3). Leaf mass per unit area, conversely, was high during the middle of the season where leaves were structurally mature, and declined at the end, in accordance with studies demonstrating a positive correlation between leaf age and LMA during the growing season prior to senescence (Grassi et al. 2005, Hikosaka et al. 2007, Wright et al. 2006).

The seasonal change in photosynthesis seen here appears to be driven by climatic factors rather than photoperiod. The lower temperatures and VPD, accompanied by higher RWC, are correlated with an increase in g_s and increased photosynthetic rate and capacity enabling *Q. coccinea* to maximize carbon gain in advance of leaf senescence and over-wintering (Figures 2–4). Relationships between the meteorological data and $V_{c,max,25}$ presented in this study are shown in Figure S2 (available as Supplementary Data at *Tree Physiology Online*). Several previous studies have demonstrated strong effects of environmental factors on photosynthesis, in a range of species (e.g., Choat et al. 2006, Ellsworth 2000, Grassi et al. 2005, Kosugi and Matsuo

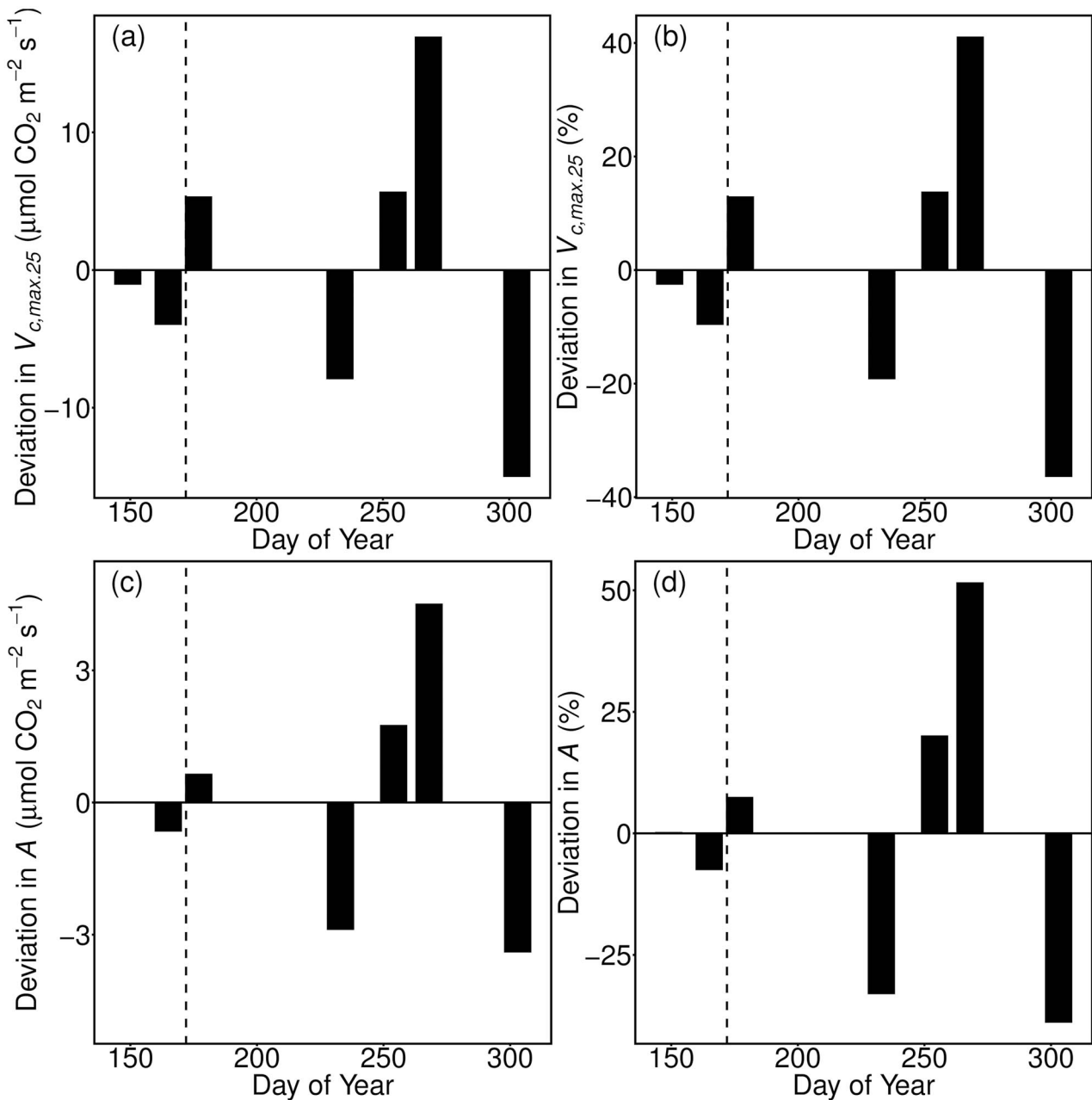


Figure 6. Both the maximum carboxylation capacity of Rubisco ($V_{c,max,25}$) and modeled photosynthesis (A) at the top of the canopy deviate from the mean, with deviation increasing as the measurement season progresses. The horizontal black line ($y = 0$) indicates the mean value of $V_{c,max,25}$ or A . The midsummer solstice is indicated with a dashed line. (a) Absolute deviation in $V_{c,max,25}$; (b) percentage deviation in $V_{c,max,25}$; (c) absolute deviation in modeled A ; (d) percentage deviation in modeled A .

2006). These responses vary between species; for example, a comparison of evergreen and deciduous species in Australia highlighted the greater sensitivity of photosynthesis in deciduous trees to dryness (Choat et al. 2006). Furthermore, it should be noted that in addition to seasonal trends in environmental factors throughout the growing season, the environment at the time of leaf flushing can also impact physiological processes (Wujeska-Klaue et al. 2019).

Leaf senescence is accompanied by a strong decline in photosynthesis

Leaf age effects, in addition to environmental factors, vary during the growing season, with nutrient resorption being a key process affecting photosynthetic activity at the time of leaf senescence (Crous et al. 2019); ontogenetic effects impact photosynthesis throughout leaf development (Ellsworth 2000, Field and

Mooney 1983, Grassi et al. 2005, Greenwood et al. 2008, Hikosaka et al. 2007, Jach and Ceulemans 2000, Kosugi and Matsuo 2006, Wright et al. 2006). In the present study, between the penultimate and final time points, PAR and temperature decreased dramatically (Figure 2), accompanied by a sharp decrease in nitrogen, chlorophyll and PRI (Figure 3). Although values of RWC and g_s displayed relatively little change between the penultimate and the final time point (Figures 3 and 4), A_{sat} decreased sharply between the last two measurement dates leading to a decoupling of A_{sat} and g_s and a strong decrease in WUEi (Figure 4). The decrease in A_{sat} was accompanied by a sharp decline in $V_{c,\text{max},25}$ and $J_{\text{max},25}$ (Figure 4). The decline in $V_{c,\text{max},25}$ was relatively greater than the decline in $J_{\text{max},25}$, which did not drop below its previous lowest value. This might reflect the greater dependency of $V_{c,\text{max},25}$ than $J_{\text{max},25}$ on leaf nitrogen content, which decreased greatly at the final time point in line with the onset of nutrient resorption and leaf senescence (Figure 4). Moreover, leaf ontogeny interacts with the environment. An example of this interaction is that older leaves may be less susceptible to drought; one study demonstrated that year-old leaves of the evergreen loblolly pine were less affected by drought than new leaves and reached peak photosynthetic capacity earlier in the year (Ellsworth 2000), while a study of deciduous trees showed that the Gaussian trend in photosynthesis associated with changing leaf age and environmental conditions throughout the season persisted but with a reduced photosynthetic capacity, during conditions of summer drought (Grassi et al. 2005).

Photosynthetic NUE is maintained throughout the season

Photosynthetic NUE remained fairly constant throughout the measurement season, with the exception of the penultimate time point (Figure 4). The lowest NUE coincided with the lowest photosynthesis, during the hottest and driest part of the season, at which point A decreased while nitrogen remained stable, a trend that has been reported previously in the mid to late summer (Wilson et al. 2001). At the penultimate time point, photosynthetic rate and capacity increased significantly while nitrogen remained very similar compared with the preceding measurement (Figures 3 and 4), leading to a peak in NUE. This may be underpinned by the lower ambient air temperatures and lower VPD facilitating increases in RWC and g_s , allowing A_{sat} to increase (Figures 2–4). At the end of the season, values of both photosynthesis and nitrogen were very low due to the remobilization of nitrogen resources during senescence; this remobilization means that photosynthetic NUE did not decrease despite the low rate and capacity of photosynthesis (Figures 3 and 4).

Trends in nitrogen varied depending on whether nitrogen was expressed per unit mass or per unit area (Figure 3), due to the changing relationship between leaf mass and area seen in the LMA data. At the start of the season, leaves had a low LMA and

therefore a low amount of nitrogen per unit area (Figure 3), as has been found previously (Grassi et al. 2005, Hikosaka et al. 2007, Wright et al. 2006). However, the nitrogen concentration per unit mass was at its highest at the first measurement (Figure 3), as seen elsewhere (Yang et al. 2016) since leaf growth was concurrent with assembly of the photosynthetic machinery despite full leaf expansion not having been achieved. Chlorophyll, PRI and nitrogen content mimicked the trend in LMA to a large extent and this was especially the case for nitrogen (Figure 3). However, this relationship was decoupled at the final time point. While chlorophyll and nitrogen dropped sharply to their lowest levels due to the nutrient remobilization processes of leaf senescence, LMA did not decline so steeply. The tight link between nitrogen and chlorophyll (when nitrogen is expressed on a leaf area basis) likely reflects the coupling between chlorophyll for light harvesting and nitrogen for the enzymes of the Calvin–Benson cycle (in particular, Rubisco).

Implications for modeling photosynthesis

Modeled photosynthesis at the top of the canopy closely reflected $V_{c,\text{max},25}$ indicative of Rubisco limited (or RuBP saturated) photosynthesis throughout the season (Figures 4 and 5). In order to understand the constraints associated with selecting a time point for deriving model parameters, we plotted the deviation in $V_{c,\text{max},25}$ and modeled A for each measurement date (Figure 6). In each case, values early in the season, before and around the midsummer solstice, led to lower deviation from the mean than values later in the season (Figure 6). This is due to the late season peak in photosynthesis occurring before the end of season decline, which contributes large deviations in $V_{c,\text{max},25}$ and modeled A . In our analysis, these trends in photosynthetic parameters mean that we did not observe a peak in $V_{c,\text{max},25}$ and modeled A at the solstice followed by a decline; these findings therefore contrast with our hypothesis that a measurement around the solstice would lead to a large deviation from the seasonal mean. In this instance, an early-season or midsummer solstice measurement would be most appropriate for deriving a seasonal mean value of $V_{c,\text{max},25}$ or modeled A for use in carbon cycle models. While additional years of measurement are required to confirm the trend reported here, alongside continued integration of theory and practice, the surprising variation in photosynthetic capacity and rate uncovered here for *Q. coccinea* highlights the necessity of understanding the species-level and ecosystem-level responses of photosynthesis to seasonal change if accurate estimates of photosynthetic parameters are to be obtained.

Environmental conditions therefore play an important role in modulating seasonal trends in $V_{c,\text{max},25}$ with a clear need to account for seasonality (Jiang et al. 2020). While climate shapes photosynthetic capacity along optimality principles (Smith et al.

2019), variation gradients also impact physiological processes at the seasonal scale. Furthermore, environmental factors such as temperature and water availability interact with leaf ontogeny, meaning that the biological processes occurring within the plant such as leaf expansion impact the extent to which external parameters affect photosynthesis (Grassi et al. 2005, Kosugi and Matsuo 2006). We advocate moving away from the need to establish a seasonal mean value of $V_{c,max,25}$, toward a greater understanding of the factors driving seasonality in $V_{c,max,25}$. This may then be replicated in models to increase the accuracy of representation of photosynthetic capacity across seasons and years under different climatic conditions and across geographical areas.

Conclusions

We hypothesized that photosynthetic rates and capacities would be greatest at the midsummer solstice. Our findings run contrary to this hypothesis, with the greatest values of $V_{c,max,25}$, $J_{max,25}$ and A_{sat} observed at the penultimate measured time point, in late September. Contrary to our expectations, a measurement of photosynthetic traits in *Q. coccinea* taken at or around the summer solstice provides the closest estimate to the mean seasonal value and is therefore the most suitable time point for deriving model parameters for this species. However, we recommend incorporating seasonality in models for the most accurate representation. A multi-year, multi-species approach is needed to validate the trends shown here, yet our findings clearly indicate the potential for deviation from expected trends. A mid to late-season measurement of photosynthesis could lead to a dramatic over- or under-estimation of $V_{c,max,25}$ or modeled A , resulting in significant impacts in subsequent ecosystem modeling. Species- and environment-specific consideration, alongside consideration of leaf ontogeny, is necessary for accurate modeling of seasonal carbon uptake in deciduous forests.

Data and materials availability

The raw data presented in this manuscript are available online [http://ecosis.org] from the Ecological Spectral Information System (EcoSIS) at: <https://doi.org/10.21232/ujBYNxhm>.

Acknowledgments

We gratefully acknowledge Duncan Anderson, Sophie Drew, Casey Hamilton, Benjamin Miller and Ivanellis Rodriguez-Torres for assistance with data collection.

Conflict of interest

None declared.

Funding

This study was funded by the United States Department of Energy contract DE-SC0012704 to Brookhaven National Laboratory.

Authors' contributions

A.C.B., S.P.S. and A.R. conceived and designed the study. All authors contributed to methodology development, experiment execution and data collection. A.C.B. analyzed the data and wrote the manuscript with contributions from S.P.S., J.L. and A.R.

References

- Ali AA, Xu C, Rogers A et al. (2015) Global-scale environmental control of plant photosynthetic capacity. *Ecol Appl* 25:2349–2365.
- Bauerle WL, Oren R, Way DA, Qian SS, Stoy PC, Thornton PE, Bowden JD, Hoffman FM, Reynolds RF (2012) Photoperiodic regulation of the seasonal pattern of photosynthetic capacity and the implications for carbon cycling. *Proc Natl Acad Sci USA* 109:8612–8617.
- Bernacchi CJ, Singaas EL, Pimentel C, Portis AR Jr, Long SP (2001) Improved temperature response functions for models of Rubisco-limited photosynthesis. *Plant Cell Environ* 24:253–259.
- Bernacchi CJ, Pimentel C, Long SP (2003) In vivo temperature response functions required to model RuBP-limited photosynthesis. *Plant Cell Environ* 26:1419–1430.
- Bernacchi CJ, Bagley JE, Serbin SP, Ruiz-Vera UM, Rosenthal DM, Vanloocke A (2013) Modelling C3 photosynthesis from the chloroplast to the ecosystem. *Plant Cell Environ* 36:1641–1657.
- Burnett AC, Davidson KJ, Serbin SP, Rogers A (2019) The “one-point method” for estimating maximum carboxylation capacity of photosynthesis: a cautionary tale. *Plant Cell Environ* 42:2472–2481.
- Choat B, Ball MC, Lully JG, Donnelly CF, Holtum JAM (2006) Seasonal patterns of leaf gas exchange and water relations in dry rain forest trees of contrasting leaf phenology. *Tree Physiol* 26:657–664.
- Crous KY, Wujeska-Klaus A, Jiang MK, Medlyn BE, Ellsworth DS (2019) Nitrogen and phosphorus retranslocation of leaves and stemwood in a mature *Eucalyptus* forest exposed to 5 years of elevated CO₂. *Front Plant Sci* 10:13.
- De Kauwe MG, Lin YS, Wright IJ et al. (2016) A test of the ‘one-point method’ for estimating maximum carboxylation capacity from field-measured, light-saturated photosynthesis. *New Phytol* 210:1130–1144.
- Ellsworth DS (2000) Seasonal CO₂ assimilation and stomatal limitations in a *Pinus taeda* canopy. *Tree Physiol* 20:435–445.
- Field C, Mooney HA (1983) Leaf age and seasonal effects on light, water, and nitrogen use efficiency in a California shrub. *Oecologia* 56:348–355.
- Gamon JA, Serrano L, Surfus JS (1997) The photochemical reflectance index: an optical indicator of photosynthetic radiation use efficiency across species, functional types, and nutrient levels. *Oecologia* 112:492–501.
- Grassi G, Vicinelli E, Ponti F, Cantoni L, Magnani F (2005) Seasonal and interannual variability of photosynthetic capacity in relation to leaf nitrogen in a deciduous forest plantation in northern Italy. *Tree Physiol* 25:349–360.
- Greenwood MS, Ward MH, Day ME, Adams SL, Bond BJ (2008) Age-related trends in red spruce foliar plasticity in relation to declining productivity. *Tree Physiol* 28:225–232.

- Hikosaka K, Nabeshima E, Hiura T (2007) Seasonal changes in the temperature response of photosynthesis in canopy leaves of *Quercus crispula* in a cool-temperate forest. *Tree Physiol* 27:1035–1041.
- Jach ME, Ceulemans R (2000) Effects of season, needle age and elevated atmospheric CO₂ on photosynthesis in scots pine (*Pinus sylvestris*). *Tree Physiol* 20:145–157.
- Jiang C, Ryu Y, Wang H, Keenan T (2020) An optimality-based model explains seasonal variation in C3 plant photosynthetic capacity. *Glob Chang Biol* 26:6493–6510.
- Kamoske A, Dahlin K, Serbin S, Stark S (2020) Leaf traits and canopy structure together explain canopy functional diversity: an airborne remote sensing approach. *Ecol Appl*. 31:e02230. doi: [10.1002/eap.2230](https://doi.org/10.1002/eap.2230).
- Kattge J, Knorr W, Raddatz T, Wirth C (2009) Quantifying photosynthetic capacity and its relationship to leaf nitrogen content for global-scale terrestrial biosphere models. *Glob Chang Biol* 15:976–991.
- Knauer J, El-Madany T, Zaehle S, Migliavacca M (2018) Bigleaf - an R package for the calculation of physical and physiological ecosystem properties from eddy covariance data. *PLoS One* 13:e0201114. doi: [10.1371/journal.pone.0201114](https://doi.org/10.1371/journal.pone.0201114).
- Kosugi Y, Matsuo N (2006) Seasonal fluctuations and temperature dependence of leaf gas exchange parameters of co-occurring evergreen and deciduous trees in a temperate broad-leaved forest. *Tree Physiol* 26:1173–1184.
- Koven CD, Knox RG, Fisher RA et al. (2020) Benchmarking and parameter sensitivity of physiological and vegetation dynamics using the functionally assembled terrestrial ecosystem simulator (FATES) at Barro Colorado Island, Panama. *Biogeosciences* 17:3017–3044.
- Lin YS, Medlyn BE, Duursma RA et al. (2015) Optimal stomatal behaviour around the world. *Nat Clim Chang* 5:459–464.
- Long SP, Bernacchi CJ (2003) Gas exchange measurements, what can they tell us about the underlying limitations to photosynthesis? Procedures and sources of error. *J Exp Bot* 54:2393–2401.
- Medlyn BE, Duursma RA, Eamus D et al. (2011) Reconciling the optimal and empirical approaches to modelling stomatal conductance. *Glob Chang Biol* 17:2134–2144.
- Meng R, Wu J, Schwager KL, Zhao F, Dennison PE, Cook BD, Brewster K, Green TM, Serbin SP (2017) Using high spatial resolution satellite imagery to map forest burn severity across spatial scales in a pine barrens ecosystem. *Remote Sens Environ* 191:95–109.
- Muir CD (2019) Tealeaves: an R package for modelling leaf temperature using energy budgets. *AoB Plants* 11:1–10.
- R Development Core Team (2019) R: A language and environment for statistical computing. R Foundation for Statistical Computing, Vienna, Austria. <https://www.R-project.org/>.
- Richardson AD, Duigan SP, Berlyn GP (2002) An evaluation of noninvasive methods to estimate foliar chlorophyll content. *New Phytol* 153:185–194.
- Rogers A, Serbin SP, Ely KS, Sloan VL, Wullschlegel SD (2017) Terrestrial biosphere models underestimate photosynthetic capacity and CO₂ assimilation in the Arctic. *New Phytol* 216:1090–1103.
- Serbin SP, Singh A, McNeil BE, Kingdon CC, Townsend PA (2014) Spectroscopic determination of leaf morphological and biochemical traits for northern temperate and boreal tree species. *Ecol Appl* 24:1651–1669.
- Smith NG, Keenan TF, Colin Prentice I et al. (2019) Global photosynthetic capacity is optimized to the environment. *Ecol Lett* 22:506–517.
- USDA (2019) Fire Effects Information System. (Last accessed date August 2020). <https://www.feis-crs.org/feis/>
- Wang Q, Iio A, Kakubari Y (2008) Broadband simple ratio closely traced seasonal trajectory of canopy photosynthetic capacity. *Geophys Res Lett* 35:1–5.
- Wilson KB, Baldocchi DD, Hanson PJ (2000) Spatial and seasonal variability of photosynthetic parameters and their relationship to leaf nitrogen in a deciduous forest. *Tree Physiol* 20:565–578.
- Wilson KB, Baldocchi DD, Hanson PJ (2001) Leaf age affects the seasonal pattern of photosynthetic capacity and net ecosystem exchange of carbon in a deciduous forest. *Plant Cell Environ* 24:571–583.
- Wright IJ, Leishman MR, Read C, Westoby M (2006) Gradients of light availability and leaf traits with leaf age and canopy position in 28 Australian shrubs and trees. *Funct Plant Biol* 33:407–419.
- Wu J, Rogers A, Albert LP, Ely K, Prohaska N, Wolfe BT, Oliveira RC, Saleska SR, Serbin SP (2019) Leaf reflectance spectroscopy captures variation in carboxylation capacity across species, canopy environment and leaf age in lowland moist tropical forests. *New Phytol* 224:663–674.
- Wu J, Serbin SP, Ely KS et al. (2020) The response of stomatal conductance to seasonal drought in tropical forests. *Glob Chang Biol* 26:823–839.
- Wujeska-Klaue A, Crous KY, Ghannoum O, Ellsworth DS (2019) Lower photorespiration in elevated CO₂ reduces leaf N concentrations in mature *Eucalyptus* trees in the field. *Glob Chang Biol* 25:1282–1295.
- Xu L, Baldocchi DD (2003) Seasonal trends in photosynthetic parameters and stomatal conductance of blue oak (*Quercus douglasii*) under prolonged summer drought and high temperature. *Tree Physiol* 23:865–877.
- Yang X, Tang J, Mustard JF, Wu J, Zhao K, Serbin S, Lee JE (2016) Seasonal variability of multiple leaf traits captured by leaf spectroscopy at two temperate deciduous forests. *Remote Sens Environ* 179:1–12.